Nanoscale

Accepted Manuscript

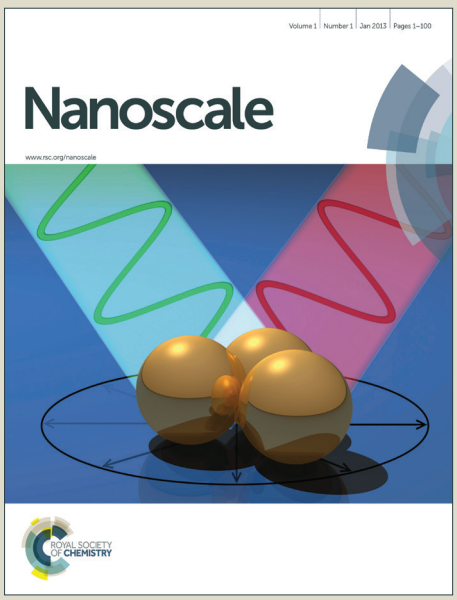

ROYAL SOCIETY OF CHEMISTRY

www.rsc.org/nanoscale

New Synthesis of Two-Dimensional CdSe/CdS core@shell Dot-in-Hexagonal Platelet Nanoheterostructures with Interesting Optical Properties

*Himani Chauhan, Yogesh Kumar, Sasanka Deka**

Department of Chemistry, University of Delhi, North campus, Delhi-110007, India

E-mail: ssdeka@gmail.com

Abstract: A new synthesis strategy for fluorescent monodispersed 2-dimensional (2D) CdSe/CdS core/shell hexagonal platelet nanocrystals has been demonstrated. Due to the stronger affinity of -NH_2 group of oleylamine to the (0001Se) facet comprising three dangling bonds in CdSe seeds, oleylamine acts as the sole responsible surfactant to hinder the growth of CdS shell in 0001 and $000\bar{1}$ facets and helps the shell growth anisotropically in <100> direction. The as-synthesized products were thoroughly characterized using XRD, TEM/HRTEM, HAADF and STEM techniques for the knowledge of crystal structure, growth mechanism and the position of seed inside a core/shell nanocrystal. Optical absorption, PL, PLE and TRPL studies revealed efficient photoexcitation and possibility of polarized emission from the 2D core/shell nanocrystals.

Keywords: 2-dimensional nanocrystal; core/shell; semiconductor; heterostructure; photoexcitation and polarized emission.

1. Introduction

The quantum-mechanical behavior of electrons in a two-dimensional (2D) system is the origin of many important physical effects, because charge carriers (electrons and holes) can move freely parallel to the semiconductor layer (x-y directions), but their movement perpendicular to the interface is restricted. In the case of nanoscale engineering, strong one-

dimensionally (1D) quantum confinement 2D semiconductor nanocrystals (I-VI and II-VI) have been realized recently.[1-5] The study of such nanostructures is important, as 2D systems already led to the discovery of remarkable 2-dimensional quantized effects, such as the Integer and the Fractional Quantum Hall Effect.[6] Moreover, important technologies have been commercialized based on 2D systems, such as, quantum well/cascade laser and detector,[7] spin valves,[8] etc. On the contrary, technologically important core/shell or double shell nanocrystals (NCs) of semiconductors are available either in 0 or 1 dimensional shape.[9-18] The protection over the core by the shell material to form either Type-I or Type-II core/shell leads to the fine tuning of emission wavelength, polarized light and more importantly the photoexcitation for photovoltaic applications. Therefore, the development of 2D core@shell nanocrystal system is highly necessitated to understand the nanoscale building blocks of 2D crystal structures and the optical properties efficaciously.

In the available literature on CdSe/CdS nanocrystal system, only few reports could be found by the authors on the synthesis of 2D core@shell system. Where Cassette et al.[19] developed dot-in-plate core/shell NCs from spherical CdSe seeds and Prudnikau et al.[20] developed wing type CdSe/CdS NCs from 2D platelet seeds by slow addition of Cd/S precursors to the preformed seeds in non-coordinating solvent (1-octadecene) environment. Later on colloidal core/crown CdSe/CdS nanoplatelets and atomically flat CdSe/CdZnS type nanoplatelets have been developed.[21,22] Extensively such a system could be termed as dot-in-plate or nanoheteroplatelet system, where a quantum dot is confined in a 2D shell nanocrystal. Based on these facts, we have developed 2D CdSe/CdS hexagonal platelet shaped core/shell nanocrystals system following a new hot injection method, where a CdSe quantum dot is confined in a 2D hexagonal platelet shell. Here we report a colloidal seeded growth synthesis strategy to

synthesize 2D CdSe/CdS hexagonal core/shell system using oleylamine, phosphonic acids and trioctylphosphine oxide by a high temperature rapid injection method to ensure the quality and crystallinity of the final product. Present method is entirely different from the earlier two reports on 2D core/shell[19,20] in terms of rapid injection, no use of starting 2D platelet template and tuning of the shell layers more efficiently just by selecting appropriate core size or shell precursor concentrations. The optical properties of the as-synthesized materials were studied thoroughly.

A two-step seed mediated synthesis strategy has been followed by manipulating the surfactants to synthesize the 2D core/shell nanoheterostructure. A schematic diagram of the synthesis is shown in Scheme 1. We have planned for two types of seeds, targeting major differences in oleylamine (OLAM) and trioctylephosphine (TOP) capping. Literature studies evidenced that the wurtzite CdSe quantum dots comprise of three predominant facets, viz. (100), $(0\bar{1}0)$ and (001). Where polar facets are 0001Cd, 0001Se, $000\bar{1}$Cd and $000\bar{1}$Se terminated.[23,24] Considering the advantages of these facts, Carbone et al.[14] and Talapin et al.[15] have independently developed anisotropic 1D nanorods of CdSe/CdS core/shell system by terminating the growth in <100> directions in terms of facet selective surfactant, such as n-hexylphosphonic acid (HPA). The z-axis of the wurtzite CdS shell, which is predominantly consist of (001) planes grow longer due to presence of sufficient Cd and S precursors. Based on these realisms we have planned to introduce another surfactant, which has stronger affinity towards Se or S in the 0001 and $000\bar{1}$ facet than HPA. Earlier reports showed that oleylamine has stronger affinity towards Se/S via electrostatic interaction and can reduce them to Se^{2-} and S^{2-}, respectively.[25-27] Thus one can consider that, addition of OLAM during the core/shell synthesis, $-NH_2$ group will strongly bind to the (0001Se) facet comprise of three dangling bonds.[25] If this interaction is stronger than

HPA-{100} facet interaction, then the CdS shell growth on the 0001 facet will be terminated (full coverage of polar facet)[24] and the available Cd and S precursors will move towards (100) surface. Hence we should see shell growth along x- and y-axis, no growth or reduced growth along z-axis, leading to anisotropic 2D hexagonal type core/shell nanoheterostructure. Keeping this in mind we have first started with the synthesis of two types of CdSe seeds as shown in step-*a* of Scheme 1, where CdSe-A seed has trioctylphosphine oxide (TOPO), OLAM and oleic acid (OLAC) as surfactants and the CdSe-B seed has TOPO, ODPA and TOP as surfactants. The second step-b is a modified seeded-growth approach from literature[14,15] for the synthesis of cadmium chalcogenide nanocrystals with controlled shapes and chemical composition and with narrow distributions of geometrical parameters, where we have carefully adjusted the amount and introduced OLAM as an additional surfactant and no use of TOP. Based on the above hypothesis, we have developed CdSe/CdS 2D nanoheteroplatelet system and obtained appreciable photoexcitation and 2D-polarized emission from the as-synthesized products.

The present paper demonstrates the new synthesis of CdSe/CdS 2D nanoheteroplatelet system as per the strategy shown in Scheme 1 and their interesting optical properties. In a typical synthesis, the usable seeds were redispersed in oleylamine and required amount of these seeds (original concentration 4.34 10^{-4} M, see supporting information for estimation) were mixed with a 0.8 mmol S/OLAM solution. This resulting CdSe/OLAM/S mixture was then injected rapidly (~0 sec) using a syringe into a flask containing a solution of cadmium alkylphosphonate (a mixture of hexylphosphonate and octadecylphosphonate) in trioctylphosphine oxide (TOPO) and OLAM under nitrogen atmosphere at 335 ^{o}C (see supporting information for synthesis details). The synthesis was allowed to run for 3-7 min at that temperature and collected the product at room temperature after precipitated by adding methanol and purified by centrifugation. Further it

is demonstrated that, oleylamine acts as a shape directing surfactant. Later from control synthesis it was confirmed that oleylamine bind strongly to Se/S of 0001 and 0001 facet to hider the shell growth in z-axis and direct the shell growth in lateral direction, i.e. in <100> direction leading to 2D dot-in-platelet or nanoheteroplatelet structure. The shell growth in terms of size can easily be tuned. Syntheses of core/shell 2D particles ranging from 10 nm to 25 nm in width are shown in the present work. Observation of self-assembly of many particles laying on their edges/side planes is also demonstrated. From the STEM measurement we confirmed the position of CdSe seed at the center of the hexagonal platelet particle, leading to equal growth distribution of CdS shell. Interesting optical properties have been observed from the nanoheteroplatelet system when it is characterized with UV-Vis, PL, PLE and TRPL measurements at room temperature. The PLE behavior of our samples has been compared to non-core/shell CdSe 2D systems, which also indicates the presence of moderate 2D-polarized emission from the present 2D core/shell particles due to only one dimensional confinement of the excitons. Again, for the first time we have carried out time-resolved fluorescence spectroscopy (TRPL) on our 2-dimensional core/shell system and here reported few of the new observations which have not been observed earlier.

2. Experimental Section

Chemicals: Cadmium oxide (CdO, 99.5%), oleic acid (OLAC, 90%), oleylamine (OLAM 70%), 1-octadecene (ODE, 90%) and trioctylphosphine oxide (TOPO, 99%) were purchased from sigma Aldrich, USA. Selenium powder (Se, 99.99%), sulphur powder (S, 99.99%) and trioctylphosphine (TOP, 99%) were from Strem chemicals, USA. n-Octadecylphosphonic acid (ODPA, >97%), n-hexylphosphonic acid (HPA, >97%) were purchased from PlasmaChem, Germany. Anhydrous toluene and methanol were purchased from Thomas baker, India. All

chemicals were used as received.

Synthesis of CdSe QD seeds (CdSe-A): CdO 1.0 mmol (0.128 g), oleic acid 6.3 mmol (2mL), trioctylphosphine oxide 5.17 mmol (2.0 g) and 1-octadecene 15.6 mol (5 mL) were loaded into a 50 mL three necked flask and heated to 150 ^{o}C for 1 h under vacuum. This mixture was heated to 300 ^{o}C under N_2 atmosphere. At this temperature a well dispersed solution of elemental Se (1.5 mmol, 0.118 g) in 1mL of oleylamine (from glove box under N_2 atmosphere) was injected through big needle syringe to the above mixture. Instantly heating mantle was removed at 0 second and anhydrous toluene (5 mL) was added to the reaction mixture to stop the reaction and allowed the reaction mixture to cool to room temperature. The oranges-red precipitate obtained on the addition of anhydrous methanol was centrifuged and redispersed in 1mL of anhydrous toluene or oleylamine for further use.

Synthesis of CdSe QD seeds (CdSe-B): CdSe Q.Ds. were prepared following a method available in literature.[1,2,14] CdO 0.44 mmol (0.057 g), TOPO 7.7 mmol (3.0 g) and ODPA 0.85mmol (0.283 g) was degassed at 180 ^{o}C for 1 hour in a three necked round bottom flask. Then N_2 gas was passed through this solution and temperature was increased to 370 °C. As the temperature reaches the set temperature 1.5 g of TOP was added, this decreased the temperature of Cd precursor solution. At 370 ^{o}C, elemental Se 7.35 mmol (0.58 g) dissolved in 0.359 g of TOP was injected to the Cd precursor solution with the help of big needle syringe under N_2 gas flow. Instantly heating mantle was removed at 0 sec and 5 mL of anhydrous toluene was added to stop the reaction and the reaction mixture was allowed to cool at room temperature. Anhydrous methanol was added to precipitate the product. As-obtained CdSe nanocrystals were dispersed either in 1mL of toluene or 1 mL of oleylamine.

CdSe/S/OLAM stock solution*:* Elemental S powder (1.87 mmol, 0.060g) was dissolved in

OLAM (4.0 mmol, 1.07g) in a 5mL glass vial by heating and stirring inside a glove box. 300µL of CdSe-A/OLAM or CdSe-B/OLAM solution was added to the above solution to make CdSe/S/OLAM stock solution. The concentration of CdSe NCs in 1 mL oleylamine is calculated to be 4.34 10^{-4} M.

Synthesis of CdSe@CdS core/shell nanoheteroplatelets: CdO 0.23 mmol (0.030g), TOPO 3.8 mmol (1.5g) , ODPA 0.43 mmol (0.144g) and HPA 0.24 mmol (0.04g) were taken in a three necked RB flask and degassed at 150 ^{o}C for 1 h. Temperature was increased to 335 ^{o}C under N_2 atmosphere. 1 g of oleylamine was added at this point to the above transparent mixture solution and awaited to reach the set temperature (335 ^{o}C). Either CdSe-A/S/OLAM or CdSe-B/S/OLAM stock solution was rapidly (0 sec) injected to the above solution at 335 ^{o}C. Finally the reaction was stopped at 7 min by removing heating mantle and addition of anhydrous toluene (5 mL) instantly. Methanol was added to precipitate yellowish-orange product of CdSe/CdS nanocrystals and centrifused. Finally as-obtained CdSe/CdS nanocrystals were dispersed in 1 mL of anhydrous toluene.

3. Results and Discussion

Different modes of transmission electron microscopy (TEM) have been used to analyze the morphology, topology, crystal structure and growth of the as-synthesized CdSe/CdS NCs and the images are summarized in Fig. 1. We have started with monodispersed hexagonal wurtzite CdSe-A seeds of ~4.0 nm particle size (Fig. 1a) for the shell growth. Hexagonal platelet like particles with average particle size 25 nm were observed after the growth of CdS shell over the starting CdSe seeds (Fig. 1b). CdSe/CdS nanoheteroplatelet morphology of the as synthesized samples could be further revealed by dark-field imaging of the sample as shown in Fig. 1c. More representative TEM images are given in Fig. S1. The platelet CdS shell has wurtzite crystal

structure, whose reticular (100) planes grew epitaxially with CdSe (100) planes. Distinctive sets of lattice fringes which are corresponding to reticular planes of CdS ($d_{100}^{CdS} = 0.35\,nm$) were identified using HRTEM. 2D fast furrier transform (2D-FFT) calculated from panel 'd' is shown in Fig. 1e, where the presence of other planes, for instance (110) could be identified. Moreover the phase contrast HAADF measurement (panel f) clarify the two dimensional morphology of the as-synthesized product. The platelet thickness can be measured when they stack on their edge (Fig. 1g and inset) and is found to be ~8 nm (inset: histogram), i.e. 8 x 25 nm is the thickness:width dimension in the present case. We could see very few small particles (<10 nm) in Fig. 1b,c,f,g along with the bigger core/shell particles (also see common histogram of Fig. 1b,c). These could be CdS nanoparticles, formed from homogeneous nucleation during the hot injection process. Elemental mapping via energy-filtered TEM (Fig. 1h-k) confirmed that both Cd and S were uniformly distributed among the nanocrystals and Se at the center (green dots), which means that there was no appreciable compositional variation among them. However, we observed less amount of Se, which is admittedly because of the presence of Se only at the core (see EDAX spectra in Fig. S2).

The size of the core/shell nanoheteroplatelet structure in the lateral direction could be tuned either using variable sizes of the starting cores or by changing parameters such as the amount of Cd/S precursors. In four different shell growth syntheses we have started with CdSe-A cores of different sizes but with same seed particle concentration keeping the Cd/S precursors concentrations intact and the resulting particle images are shown in Fig. 2. The effect of use of increasing size of the cores (reduction in heteronucleation center) could be corroborated from the TEM images, where average particle size (width, edge to edge) of the final product increases from 13 nm to 25 nm. At the same time the thickness of the 2D particles raised by 4 nm (panel a

to panel d), however, this thickness enhancement is negligible as compared to the size enhancement in lateral dimensions. Ithurria et al. demonstrated that, in the case of CdSe nanoplatelet when the thickness is around few monolayers, the lateral dimensions could range from 20 nm to a few hundred nanometers. Thus, in the present case even though the lattice mismatch of $CdSe_{100}$ and CdS_{100} plane is about 5%, the calculated numbers of CdS layers over CdSe seeds in lateral direction were found to be 24-67 for these 2D nanocrystals. Such control over size is important for the 2D-polarized emission and efficient photoexcitation properties.

The crystal phase of the starting seeds and the final core/shell has been further identified using powder XRD measurements. The comparative XRD patterns of the seeds (CdSe-A, and CdSe-B) and the corresponding core/shell structures are depicted in Fig. 3 along with the bulk XRD patterns. The method followed to synthesize CdSe-A cores usually gives zinc-blend CdSe crystal structure at low temperature synthesis.[15,28,29] However there could be a phase transition to wurtzite if the synthesis is carried out at high temperature (300 ^{o}C, present case). Therefore, we observed hexagonal CdSe in our sample by observing (102) and (103) planes and absence of zinc-blend (400) planes at the respective 2θ values. This result is corroborated with the HRTEM analysis (inset of Fig. 1a), where only (002) planes of wurtzite structure were visible. On the other hand CdSe-B is always wurtzite as evidenced from literature.[14,15,30] Shift in the peak position towards higher 2θ was observed for the core/shell system, where peaks only from CdS were observed. Intense (110) and (100) *hkl* planes further confirmed the growth of the shell in 2D direction (x- and y-axis), rather than (002) planes for nanorods.

As mentioned earlier, we have performed another core/shell synthesis with core CdSe-B (~3 nm) to examine the formation of 2D-nanoheteroplatelet structure with TOP capped CdSe seed rather than preferentially OLAM capped CdSe-A cores. TEM analyses of the final

core/shell sample are illustrated in Fig. 4. Interestingly, formation of monodispersed 2D platelets observed in this case as well (Fig. 4a,b). To clarify further the presence of CdSe seed inside the CdS shell, we have carried out HAADF-STEM analysis and the corresponding images are shown in Fig. 4c,d. The STEM analysis of a 30 nm platelet shows the presence of minute amounts Se elements along with large amounts Cd and S elements depicting the retainment of the starting CdSe seed inside the hexagonal platelet structure. Under the HRTEM imaging of a single crystalline particle (Fig. 4e, corresponding profile plot and 2D-FFT are shown in inset), only (1000) planes of wurtzite CdS could be unambiguously identified where the shell growth took place in *a* and *b* directions. Fig. 4f-i shows the distribution of Cd, S and Se from a group of 2D core/shell NCs.

From the above discussions, it becomes clear that with the present core/shell synthesis method it is possible to synthesize CdSe/CdS 2D-nanoplatelets using at least two types of CdSe seeds. Now to clarify the role of OLAM on the formation of platelet morphology as claimed in the scheme, we have carried out few control syntheses and the results are shown in Table 1 (see supporting information for corresponding TEM images and XRD patterns, Fig. S3-4). Interestingly no 2D-hexagonal platelet shapes observed when the core/shell synthesis was carried out in absence of OLAM (reaction-1). With the help of OLAM we could get the similar shape even in the absence of TOPO or ODPA/HPA mixture or Cd or S precursors (reaction 2-4). Important to note that, monodispersed nanorods observed when we followed the core/shell synthesis method using either CdSe-A or CdSe-B cores as reported earlier.[14,15] Thus it is confirmed that OLAM has selectivity towards {001} and $\{00\bar{1}\}$ facets and actively prefer those corresponding surfaces and hinder growth along z-axis, implying its role on the topological growth of the nanoheteroplatelet in 2 dimension. Moreover, the proof of epitaxial growth of CdS

along <100> direction of CdSe seed could be ascertain from the control reaction no 5, where no seeds were injected during the synthesis. Absence of wurtzite seeds leads to random shapes of CdS nanostructures.

The overgrowth of CdS shell over the CdSe seed was examined by monitoring the optical absorption (UV-Vis), photoluminescence (PL) and photoluminescence excitation (PLE) spectra as shown in Fig. 5a,b. It could be demonstrated that the PL spectrum is red shifted on the formation of CdS shell over CdSe seeds as the delocalization of the electron in the intact core/shell system takes place where as the holes remained localized in the seed CdSe.[9-18] PLE study was done on exciting NCs in red region of the PL band ($\lambda_{em(CdSe)}$ = 565 nm and $\lambda_{em(CdSe/CdS)}$ = 621nm). PLE spectra of both CdSe core and CdSe/CdS core shell NCs follow the same pattern as the absorbance spectra respectively. The nearly resemblance of PLE spectrum to their corresponding absorbance spectrum points to formation of nanohetrogeneous structure with efficient charge and energy transfer.[20] The higher energy portion (< 500 nm) of PLE and absorption spectrum is the contribution from thick CdS shell. However, a minor discrepancy of these two spectra observed in this higher energy portion may be due to the presence of few small homogeneously nucleated CdS particles. Interestingly, PL spectrum of our core/shell sample is broader than the corresponding core but with equal intensity (optical density of all samples kept at 0.08). This behavior could be related to the confinement of the excitons only in 1 dimension, rather than 2 or 3 dimensions in the case of nanorods or Q.Ds., respectively. As reported earlier in the case of wavelength dependent 2D-polarized emission, in the present case also a splitting of the first excitonic peak (in PLE, Fig. 5b) is observed due to the splitting between the heavy hole and light hole bands.[19,31] Further, on increasing the number of shell layers from 21 to 27, enhanced splitting in PLE spectrum is observed (Fig. S5) suggesting a possibility of having

strong polarized emission in 2dimensions. This observed splitting in first excitation peak, which splits to two weak shoulders (595 nm and 605 nm for 14 nm; 597 nm and 603 nm for 12 nm core/shell particles respectively) is due to the transition ($1S_{3/2} - 1S_e$) which is generated from the crystal anisotropy (formation of heterostructure core/shell). Thus it can be concluded that the additional splitting of heavy hole and light hole (transition) is due to anisotropic pressure of CdS shell on CdSe core.[19,21] Absorption, PLE and PL bands in the present sample are maximum red shifted (46 meV) lower in magnitude as compared to nanorod or 2D core/shell samples,[19,32] but in higher magnitude as compared to CdSe-CdS wing samples.[20] Moreover, the position of emission could be easily tuned by controlling the shell growth time (Fig. S6). This kind of PL red-shift behavior already extensively demonstrated for type I and type II core/shell structure by various research groups,[11-20,33,34] which is due to a decrease in charge carrier's confinement energy. However, in the present case enhanced splitting in PLE spectrum and red-shift in emission with increasing numbers of shell layers together may be attributed to the 2D confinement organization of electrons and holes in 2D NCs, which points out the efficient photoexcitation of the hexagonal platelet nanoheterostructures.

In order to understand the relaxation dynamics of the excited electrons for the first time in 2D nanoheterostructures, TRPL spectroscopy measurement has been performed on diluted solutions. Obtained decay curves were fitted to biexponential model and shown in Fig. 5c.The average life time of NCs is calculated by expression (1)[35]

$$\tau_{av} = (B_1\tau_1{}^2 + B_2\tau_2{}^2)/(B_1\tau_1 + B_2\tau_2) \quad (1)$$

Where τ_1 and τ_2 are short lived (or fast) and long lived (or short) component respectively, and B_1 and B_2 are amplitudes of components respectively. Short term lived component (τ_1) represents life time of fluorescence decay at the band edge comprised of both radiative decay from electron-

hole recombination.[36] However, our CdSe core having τ_1 and τ_2 of 5 ns and 20 ns and that for CdSe/CdS NCs was of 6 ns and 21 ns respectively. Average life time decay τ_{av} was found 17 ns for CdSe and 20 ns for respective CdSe/CdS core shell on biexponentail curve fitting of the decay curve. The average radiative lifetime (τ_{av}), referred to as the time at which the PL signal is reduced by a 1/*e* factor, is a bit higher in the case of CdSe/CdS hexagonal NCs than the CdSe core may be due to the presence of probable trap states on two terrace faces where the presence of CdS shell layer is negligible and the consequent delocalization of the excited electrons. Moreover, a low value quantum yield of the 2D CdSe/CdS (20%) than the CdSe core (25%) can be justified by surface-related trap states in the former one acting as faster non-radiative de-excitation channels for photogenerated charge carriers and less number of CdS shell layers in z-direction (001).

4. Conclusion

In conclusion, we have demonstrated a new method to prepare 2D CdSe/CdS core/shell nanostructure system using differentially capped CdSe cores. In this novel synthesis strategy oleylamine plays the crucial role in determining the core/shell morphology to 2-dimensional by hindering the growth in z-direction. Fine tuning of width of the final products could be done by adjusting either initial core size or by shell precursors. Absorption, PL, PLE and TRPL studies show efficient PL excitation contribution and plausible polarized emission from the as-synthesized nanoheteroplatelet system.

Acknowledgements

This work was supported by BRNS-DAE research fund (grant no. 2011/20/37P/11/BRNS/1733). H.C. thanks UGC-India and Y.K. thanks BRNS-DAE for research fellowship. The authors thank USIC-DU for characterization facility.

Electronic supplementary information (ESI): Characterization procedures, additional TEM/HRTEM images, EDAX, TEM/XRD patterns of control reaction products, PLE of tuning of shell growth, PL spectra with shell growth time.

References

1. S. Ithurria, G. Bousquet and B. Dubertret, *J. Am. Chem. Soc.*2011, **133**, 3070.
2. Z. Li and X. Peng, *J. Am. Chem. Soc.*2011, **133**, 6578.
3. K. P. Rice, A. E. Saunders and M. P. Stoykovich, *J. Am. Chem. Soc.*2013, **135**, 6669.
4. H. Li, R. Brescia, M. Povia, M. Prato, G. Bertoni, L. Manna and I. Moreels, *J. Am. Chem. Soc.* 2013, **135**, 12270.
5. K. J. Koski and Y. Cui *ACS Nano* 2013, **7**, 3739.
6. D. C. Tsui, H. L. Stormer and A. C. Gossard, *Phys. Rev. Lett.* 1982, **48**, 1559.
7. T. Chakraborty and V. M. Apalkov, *Adv. in Phys*. 2003, **52**, 455.
8. S. A. Wolf, D. D. Awschalom, R. A. Buhrman, J. M. Daughton, S. von Molnár, M. L. Roukes, A. Y. Chtchelkanova and D. M. Treger, *Science* 2001, **294**, 1488.
9. B. O. Dabbousi, J. RodriguezViejo, F. V. Mikulec, J. R. Heine, H. Mattoussi, R. Ober, K. F. Jensen and M. G. Bawendi, *J. Phys. Chem. B 1997*, **101**, 9463.
10. X. Peng, M. C. Schlamp, A. V. Kadavanich and A. P. Alivisatos, *J. Am. Chem. Soc.*1997, **119**, 7019.
11. S. Kim, B.R. Fisher, H-J Eisler and M.G. Bawendi, *J. Am. Chem. Soc*. 2003, **125**, 11466.
12. H. Borchert, D. V. Talapin, C. McGinley, S. Adam, A. R. B. de Castro, T. Moller and H. Weller. *J. Chem. Phys.* 2003, **119**, 1800.
13. D. V. Talapin, I. Mekis, S. Götzinger, A. Kornowski, O. Benson and H. Weller. *J. Phys. Chem. B.* 2004, **108**, 18826.
14. L. Carbone, et al *NanoLett.* 2007, **7**, 2942.
15. D. V. Talapin, J. H; Nelson, E. V. Shevchenko, S. Aloni, B. Sadtler and A. P. Alivisatos, *NanoLett.* 2007, **7**, 2951.
16. S. Deka, A. Quarta, A. Falqui, M. G. Lupo, G. Lanzani, C. Giannini, R. Cingolani, T. Pellegrino and L. Manna, J. Am. Chem. Soc. 2009, **131**, 2948.
17. P. Reiss, M. Protière and L. Li, *Small*, 2009, **5**, 154.
18. H. Htoon, A. V. Malko, D. Bussian, J. Vela-Becerra, Y. Chen, J. A. Hollingsworth and V. I. Klimov, *NanoLett.* 2010, **10**, 2401.
19. E. Cassette, B. Mahler, J.-M. Guigner, G. Patriarche, B. Dubertret and T. Pons, *ACS Nano* 2012, **6**, 6741.
20. A. Prudnikau, A. Chuvilin and M. Artemyev, *J. Am. Chem. Soc.* 2013, **135**, 14476.
21. M. D. Tessier, P. Spinicelli, D. Dupont, G. Patriarche, S. Ithurria and B. Dubertret, *Nano Lett.*, 2014, **14**, 207.

22. B. Mahler, B. Nadal, C. Bouet, G. Patriarche and B. Dubertret, *J. Am. Chem. Soc.*, 2012, **134**, 18591.
23. J. J. Shiang, A. V. Kadavanich, R. K. Grubbs and A. P. Alivisatos, *J. Phys. Chem.* 1995, **99**, 17417.
24. L. Manna, L. W. Wang, R. Cingolani and A. P. Alivisatos, *J. Phys. Chem.B* 2005**, 109**, 6183.
25. A. Puzder, A. J. Williamson, N. Zaitseva, G. Galli, L. Manna and A. P. Alivisatos, *NanoLett.,* 2004, **4**, 2361.
26. M. Sun and X. Yang, *J. Phys. Chem. C* 2009, **113**, 8701.
27. Y. Liu, D. Yao, L. Shen, H. Zhang, X. Zhang and B. Yang, *J. Am. Chem. Soc.* 2012, **134**, 7207.
28. L. Han, D. Qin, X. Jiang, Y. Liu, L. Wang, J. Chen and Y. Cao, *Nanotechnology* 2006, **17**, 4736.
29. L. Liu, Z. Zhuang, T. Xie, Y.-G. Wang, J. Li, Q. Peng and Y. Li, *J. Am. Chem. Soc.* 2009, **131**, 16423.
30. Z. A. Peng and X. Peng, *J. Am. Chem. Soc.* 2001, **123**, 168.
31. D. B. Tice, D. J. Weinberg, N. Mathew, R. P. H. Chang and E. A. Weiss, *J. Phys.Chem.C* 2013, **117**, 13289.
32. S. Ithurria and D. V. Talapin, *J. Am. Chem. Soc.* 2012, **134**, 18585.
33. N. Gaponik, S. G. Hickey, D. Dorfs, A. L. Rogach and A. Eychmüller, *Small* 2010, **6**, 1364.
34. M. Ali, S. Chattopadhyay, A. Nag, A. Kumar, S. Sapra, S. Chakraborty and D. D. Sarma, *Nanotechnology* 2007, **18**, 075401.
35. Q. Zeng, X. Kong, Y. Sun, Y. Zhang, L. Tu, J. Zhao and H. Zhang, *J. Phys. Chem. C* 2008, **112**, 8587.
36. M. D. Garrett, A, D. Dukes III,J. R. McBride, N. J. Smith, S. J. Pennycook and S. J. Rosenthal, *J. Phys. Chem. C* 2008, **112**, 12736.

Scheme 1. Sketch of the Synthetic Procedure Devised to Synthesize the 2D core@shellnanoheterostructures.[a]

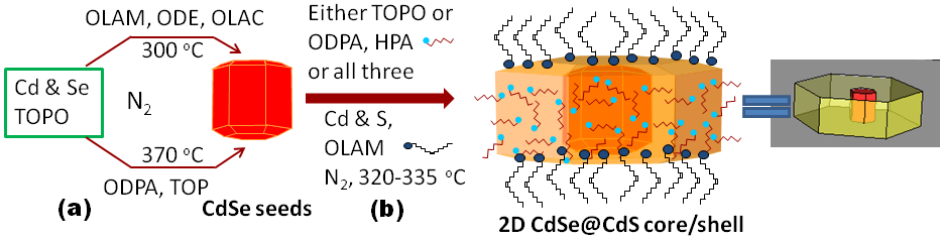

[a](a) synthesis of CdSe seeds following two different methods, (b) synthesis strategy to 2D dot-in-hexagonal platelet core/shell nanoheterostructures.

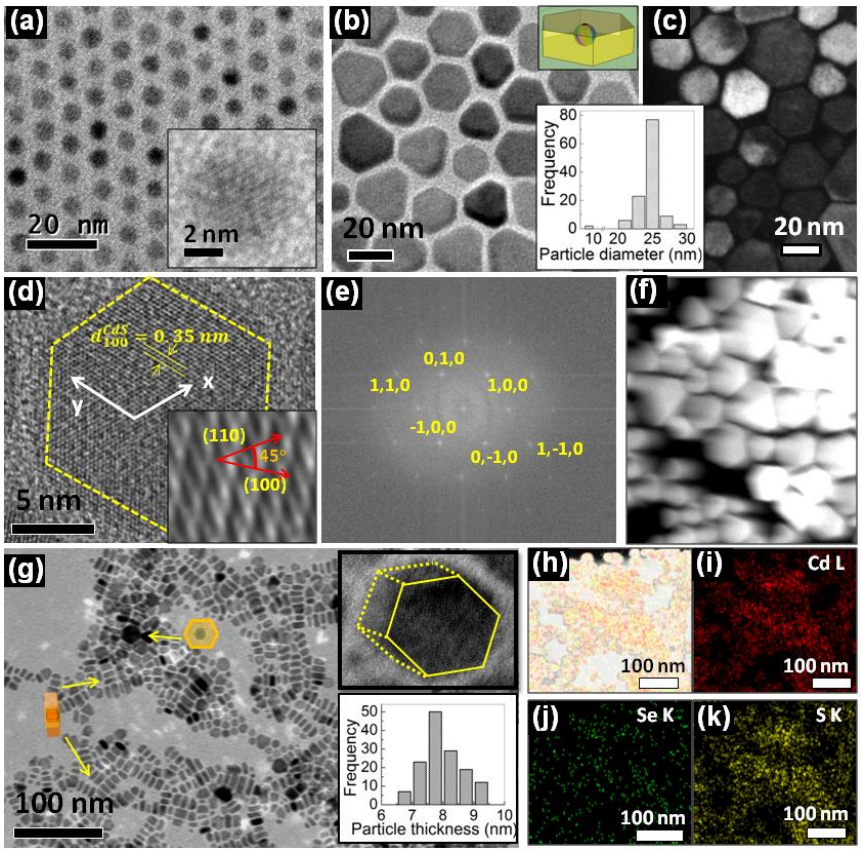

Fig. 1. (a) TEM image of CdSe-A QD seeds (inset: HRTEM image), (b) representative TEM image of CdSe/CdS 2D nanostructures obtained using CdSe-A, inset: lateral particle diameter histogram (c) dark-field TEM imaging. (d) HRTEM image showing clear lattice fringes from a single particle (inset: shows orientation of planes) and (e) is the 2D-FFT image calculated from panel 'd' (zone axis [0,0,1]). (f) HAADF (Z-contrast) image of the core/shell nanostructures. (g) Self-assembled particles lying on the edges in these sides (upper inset: a tilted particle showing 3d view with side planes, lower inset: histogram). (h) TEM elemental mapping (ZL) of a group of CdSe/CdS nanocrystals showing all three elements, (i-k) Cd, Se and S elemental maps from the same group obtained by filtering the Cd L edge, Se K edge and S K edge, respectively.

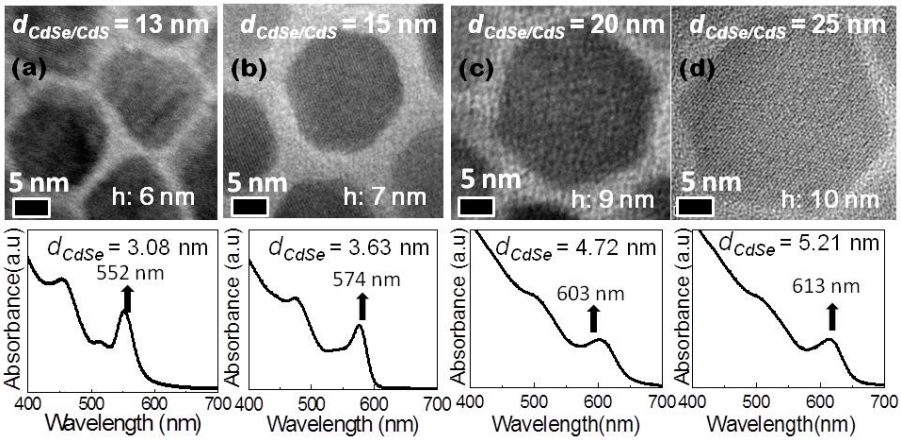

Fig. 2. HRTEM images of CdSe/CdS nanocrystals showing the tuning of size of the hexagonal CdS shell over CdSe seeds depending on the increasing size of the CdSe cores (h: thickness). Bottom panels show the absorption spectra of the corresponding CdSe cores depicting their sizes.

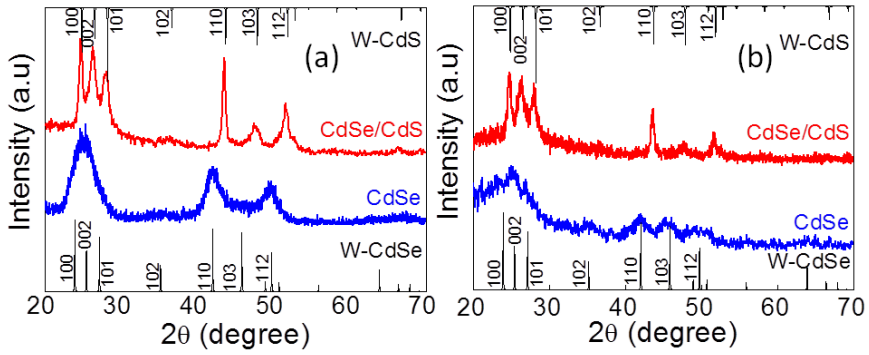

Fig. 3. Powder XRD patterns of the (a) starting core CdSe-A and final CdSe/CdS nanoheterostructure system and (b) core CdSe-B and corresponding CdSe/CdS. XRD pattern of bulk wurtzite CdSe (JCPDS card #77-2307, bottom) and CdS (JCPDS card #77-2306, top).

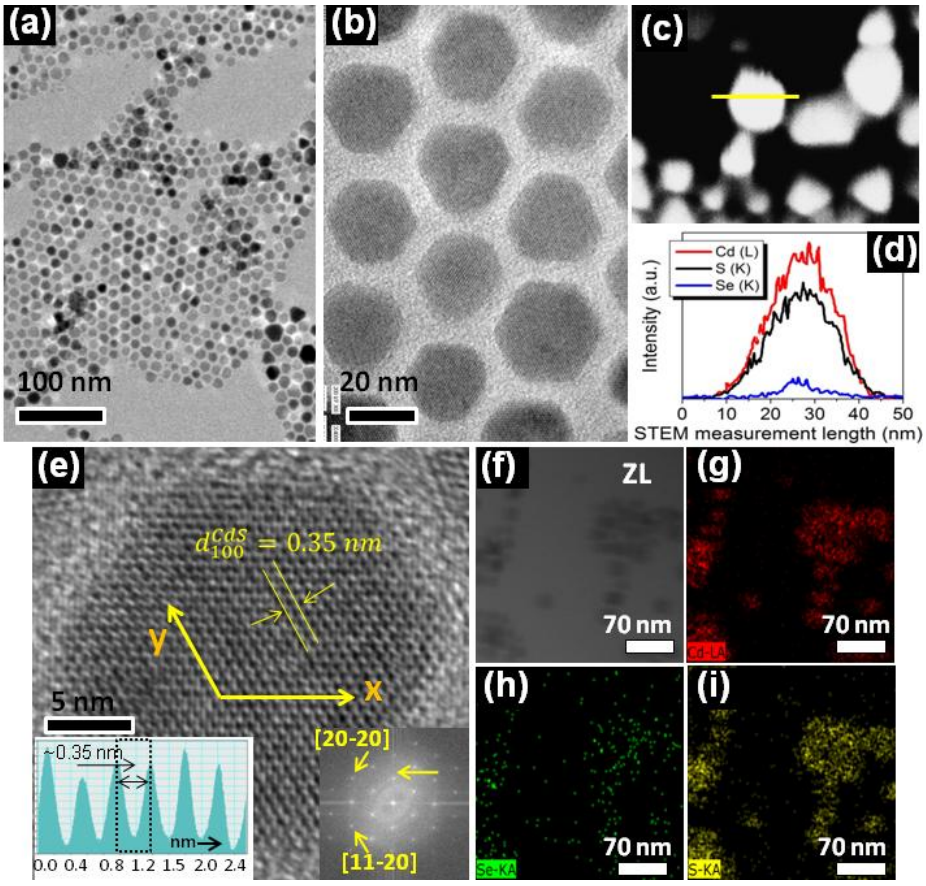

Fig. 4. TEM image of CdSe/CdS nanoheteroplatelet structure at lower (a) and at higher (b) magnifications synthesized using CdSe-B seeds. (c,d) HAADF-STEM images showing the presence of CdSe core in a CdSe/CdS core/shell nanoheteroplatelet. (e) HRTEM image of single particle showing the lateral growth directions in equivalent (1000) planes. Inset: 2D-FFT calculated from the whole particle and surface profile plot. (f) Elastic-filtered (ZL) image of several nanocrystals. (g-i) Cd, Se and S elemental maps from the same group obtained by filtering the Cd L edge, Se K edge and S K edge, respectively.

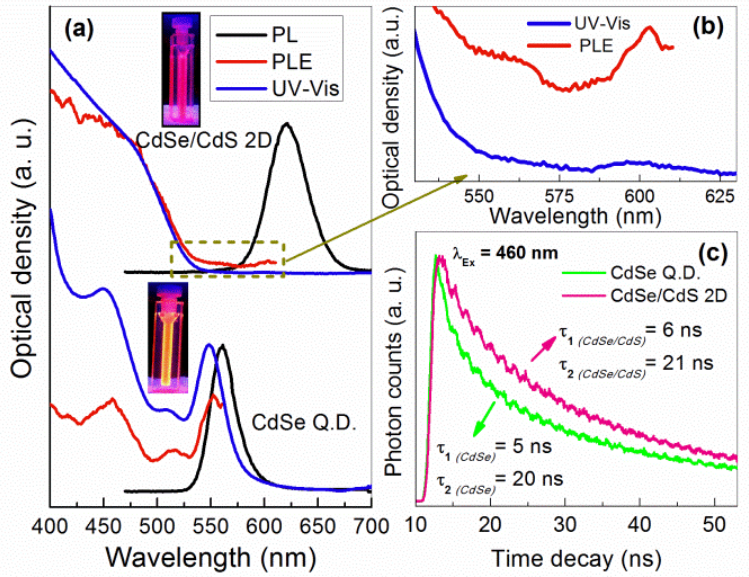

Fig. 5. (a) Optical absorption, PL and PLE spectra of colloidal core/shell dispersion in toluene and of the corresponding CdSe-B core. (b) Comparison of magnified PLE spectra part from the selected area in panel 'a'. (c) TRPL decay spectra recorded by exciting the samples at 460 nm.

Table 1. Control reactions analyses for the formation of 2D hexagonal CdSe/CdSnanocrystals.

Sl.No.	Reaction conditions					Final shape[a]
1	No OLAM	ODPA+HPA	TOPO	CdO	S	Not Hexagonal
2	OLAM	No ODPA/HPA	TOPO	CdO	S	Hexagonal
3	OLAM	ODPA+HPA	No TOPO	CdO	S	Partly Hexagonal
4	OLAM	ODPA+HPA	TOPO	No CdO or No S		Irregular/Hexagonal
5[b]	OLAM	ODPA+HPA	TOPO	CdO	S	Irregular shape
6[c]	TOP	ODPA+HPA	TOPO	CdO	S	Nanorods

[a]TEM Images and XRD patterns in supporting information, [b]No CdSe core, [c]Method for nanorods from ref. 14,15